A multi-model selection approach for statistical downscaling and bias correction of Earth System Model outputs for regional impact applications

Ricardo Oliveros-Ramos[1,2], Yunne-Jai Shin[1], Dimitri Gutierrez[2], Verena M. Trenkel[3]

[1] MARBEC, Institut de Recherche pour le Développement (IRD), Univ Montpellier, IFREMER, CNRS, Montpellier, France.

[2] Instituto del Mar del Perú (IMARPE), Lima, Perú.

[3] DECOD, IFREMER, INRAE, Institut-Agro - Agrocampus Ouest, Nantes, France.

Corresponding author: Ricardo Oliveros-Ramos (ricardo.oliveros@ird.fr)

Abstract

Earth System Models (ESMs) are the primary tool for understanding the impacts of global change and several ESMs are updated on a regular basis to provide more reliable scenarios of the future. However, the confrontation of ESMs outputs to observations reveals biases that are important to correct, especially for impact applications where the absolute scale of the environmental variable is as relevant as its trends. In addition, regional impact studies need fine scale projections to devise strategic planning and management measures. Statistical downscaling provides a fast way to produce regional ocean forcing from ESMs and can additionally produce bias-corrected outputs, which are necessary for impact applications driven by or fitted to observed data, like many ecological models. Statistical downscaling can make use of different parametric distributions depending on the variables used, and generalized regression can provide a flexible approach for this purpose. We propose a multi-model approach based on non-parametric generalized regression and a suite of indicators to select a robust statistical downscaling model that can be used for projection of future scenarios. The empirical cumulative distribution of the variables to downscale is modeled, ensuring that not only the mean but also the variance and quantiles (including the minima and maxima) are properly represented, improving the prediction of extreme events and taking into account spatial autocorrelation. The approach presented here is applied to two contrasted regional case studies, the Bay of Biscay-Celtic Sea ecosystem and the Northern Peru Current ecosystem, using the Sea Surface Temperature from the IPSL-CM5A-LR ESM. The results showed that a multi-model selection approach is appropriate as individual model performance is case specific.

1. Introduction

The primary tool for understanding the effects of climate change is Earth System Modeling, and most Earth System Models (ESM) are frequently updated to produce more accurate future scenarios. However, systematic spatio-temporal biases in ESMs outputs relative to observations have been reported (Wang et al. 2014, Cannon et al. 2015, Skogen et al. 2018, see Figure 1). Bias correction of model outputs is important for impact applications where the absolute scale of a variable is as relevant as its trends (Tabor and Williams 2010, Pourmokhtarian et al. 2016). For example, species distribution models can fail in predicting the effects of climate change scenarios if the bias in the ESMs' environmental variables produces a mismatch with the actual physiological tolerance range of the modeled species (Stoklosa et al. 2015, Morales-Barbero and Vega-Álvarez 2018). In addition, regional climate change impact studies and models need finer scale projections than those currently provided by ESMs to support strategic decision-making, evaluate management measures at the local scale (Horta and Keirstead 2016, Sugi et al. 2017), and explore adaptation and mitigation solutions. Furthermore, for some specific applications and impact studies, fine scale resolution is absolutely critical, such as water resource management, exploitation of wild species (e.g. fishing), management of wildfire risks and urbanization plans (e.g. Townhill et al. 2017, Poggio et al. 2018).

In this context, downscaling is the procedure to obtain predictions at regional scales from inputs at global or larger scales. The two main approaches to downscaling are dynamical and statistical (Hoar and Nychka 2008). Dynamical downscaling requires the simulation of a high-resolution model on a regional domain, using the lower-resolution climate model output as boundary conditions (Xu 1999, Fowler et al. 2007). These models use physical principles to reproduce regional dynamics, therefore are able to simulate local conditions in greater detail (Xu 1999, Fowler et al. 2007, Trzaska and Schnarr 2014) but are computationally intensive. Dynamical downscaling could take years of research investment, requires substantial human resources with specific technical skills and expertise in climate science, and has high performance computing costs (Fowler et al. 2007). This capacity is not found in many places in the world, yet the demand for fine resolution climate projections is ubiquitous and increases steeply for researchers. This is critical in a context where climate change scenarios and ESMs regularly change over time (and so the downscaling needs to be regularly revised), and ensemble ESMs are now available to the scientific community (and so the downscaling needs to be done multiple times). Unless strong and large multi-disciplinary teams can work hand in hand towards dynamical downscaling of climate change projections under multiple scenarios, e.g., all IPCC Representative Concentration Pathways (RCP), and potentially using multiple ESMs, researchers are often bound to use the coarse scale ESMs projections, with all the biases previously mentioned. Statistical downscaling is a two-step process consisting of i) the construction of a statistical downscaling model for the empirical relationships between regional variables and large-scale predictors, and ii) the prediction of the statistical model from the output of global climate models to simulate the regional dynamics in the future (Xu 1999, Fowler et al. 2007, Trzaska and Schnarr 2014). Statistical downscaling provides a fast way to produce regional ocean forcing from global models and can additionally produce bias-corrected outputs (e.g. Wong et al. 2014, Volosciuk et al. 2017), which are of crucial importance for impact applications driven by or fitted to observed data (e.g. most ecological models). Many statistical downscaling methods are currently available, including the combination of multiple linear regressions (e.g. Rheuban et al. 2017, Hoomehr et al. 2016, Yue et al. 2016, Hertig and Tramblay 2017, Araya-Osses et al. 2020, Bonafoni et al. 2016), machine learning (e.g. Baño-Medina et al. 2020, Anh et al. 2019, He et al. 2016, Oh et al. 2022) or ad-hoc algorithms (Han et al. 2019, Zhang et al. 2020, Keller 2017, Sa'adi et al. 2017), and parametric transformations (Lange 2019, Wang et al. 2016, Su et al. 2016, González-Aparicio et al. 2017, Huang et al. 2016). Statistical downscaling can make use of different parametric distributions depending on the variables of interest, and generalized regression can provide a flexible approach for this purpose (e.g. Asong et al. 2016, Latombe et al. 2018, Hoskins et al. 2016).

In this work, we propose a multi-model approach based on non-parametric generalized regression and a suite of indicators to select a robust statistical downscaling model that can be used for projections of future scenarios. Distribution or quantile mapping (Teutschbein and Seibert 2012, Cannon e t al. 2015) and generalized additive regression (GAMs, e.g. Latombe et al. 2018) are used to model the empirical cumulative distribution of the variables to downscale, ensuring that not only the mean but also the variance and quantiles (including the minima and maxima) are properly represented, improving the prediction of extreme events. The methods presented here are illustrated with the application to two regional case studies, the Bay of Biscay and Celtic Sea ecosystem in the Northeast Atlantic and the Northern Peru Current ecosystem in the Southeast Pacific (Figure 1). We describe our method for the Sea Surface Temperature (SST) variable outputted by the IPSL-CM5A-LR (Dufresne et. al 2013, Mignot et al. 2013) ESM.

2. Methods

The downscaling and bias correction is carried out in 7 steps:

1. Subset low resolution ESM outputs to the specific regional domain.
2. Interpolate low resolution ESM outputs to the spatial resolution of the target (observed) data.
3. Quantile computation across time for each square of the grid for both interpolated ESM outputs and target data.
4. Fit statistical models using k-fold cross validation (full dataset splitted in k equal parts).
5. Select the best models based on a suite of indicators.

6. Fit the best models selected in step 5 to the full dataset and perform final model selection based on the same suite of indicators.
7. Use the best model for prediction and produce the downscaling and bias-correction.

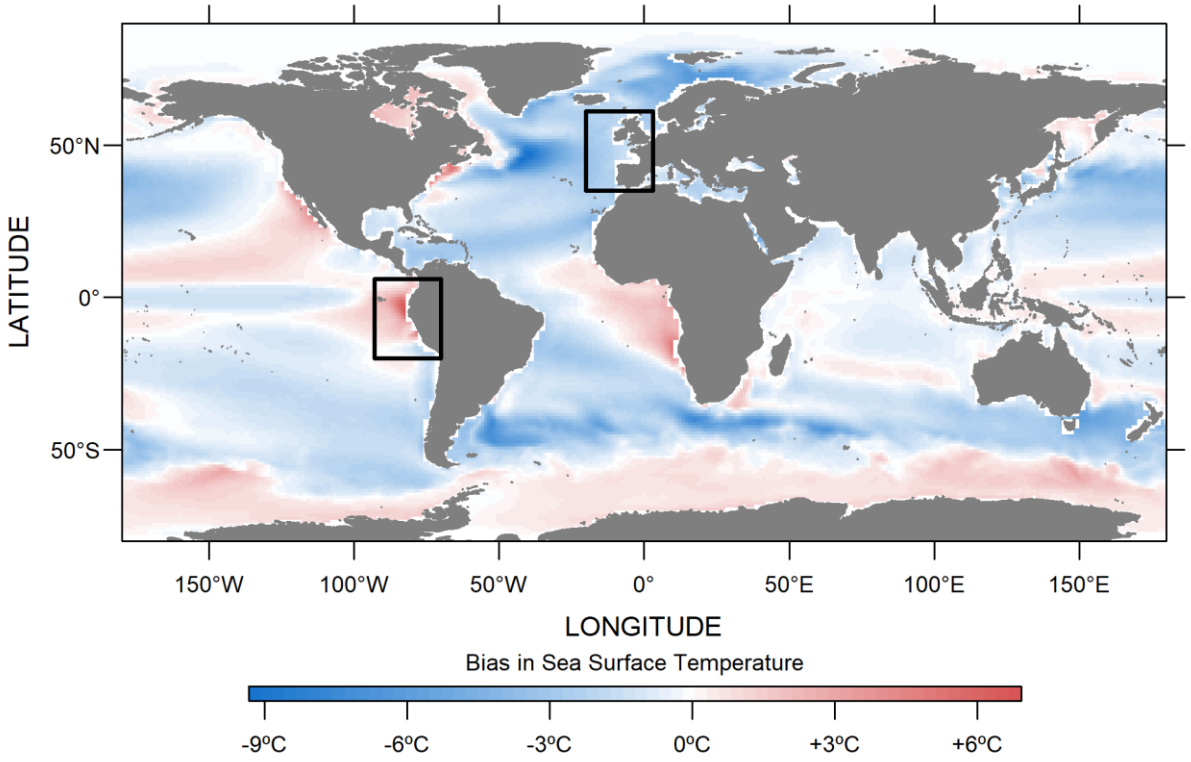

Figure 1. Bias in the average sea surface temperature in output of the IPSL-CM5A-LR model. Observations come from OI-SST (Banzon et al. 2016, Reynolds et al. 2007)

Steps 1-3 produce the databases used in the statistical modeling carried out in steps 4-6, while the final step produces the final downscaled and bias-corrected product. The approach is summarized in Figure 2 and illustrated in detail for our case studies in the next sections.

2.1 Databases

We used Sea Surface Temperature (SST) model outputs from the IPSL-CM5A-LR (Dufresne et. al 2013, Mignot et al. 2013) Earth System Model (ESM) at a spatial 1°x1° and monthly temporal resolution (ISIMIP 2a outputs, https://data.isimip.org/), for the historical period (1982-2005) and RCP 2.6 and 8.5 scenarios (2006-2100) for the climate change forecast. As target values, we used OI-SST (Banzon et al. 2016, Reynolds et al. 2007) at 0.25ºx0.25º resolution, monthly averages for the same historical period (1982-2005). ESM modeled SST was interpolated to the target resolution and grid of the OI-SST data by bilinear interpolation.

For each cell of the spatial grid, the empirical cumulative distribution of SST values during the historical period was calculated using 141 quantiles (every 0.01 in the interval [0.2, 0.8], and every 0.005 in the [0.0, 0.2[and]0.8, 1.0] intervals to improve sampling in the tails of the distribution). The data were extracted for two domains (Figure 3): The ecoregion of the Bay of Biscay and Celtic Sea (20ºW-3ºE, 35ºN-61ºN) and the Northern Peru Current ecosystem (93ºW-70ºW, 20ºS-6ºN). The data points corresponding to the Mediterranean Sea were removed from the former. A dataset with the matching quantiles for historical and future values and geolocations was constructed, including the distance to the coast and the distance to the continental shelf break (200m isobath, Figure 3), resulting in a final dataset of approximately one million records for each domain (Table 1, modeling dataset). Distance to the shelf break was log-transformed, keeping the sign (i.e. negative values inside the shelf). An identical database was constructed for the RCPs forecast data (prediction dataset). A summary of the databases is presented in Table 1.

The full historical dataset (observed and modeled) was split randomly into 24 training and validation datasets, where a bigger portion was used for validation ($1/24^{th}$ of the dataset for training and $23/24^{th}$ for validation), ensuring the totality of data was used once for training purposes. These datasets were used for model selection. The best models were fitted to the full dataset for a final model selection step.

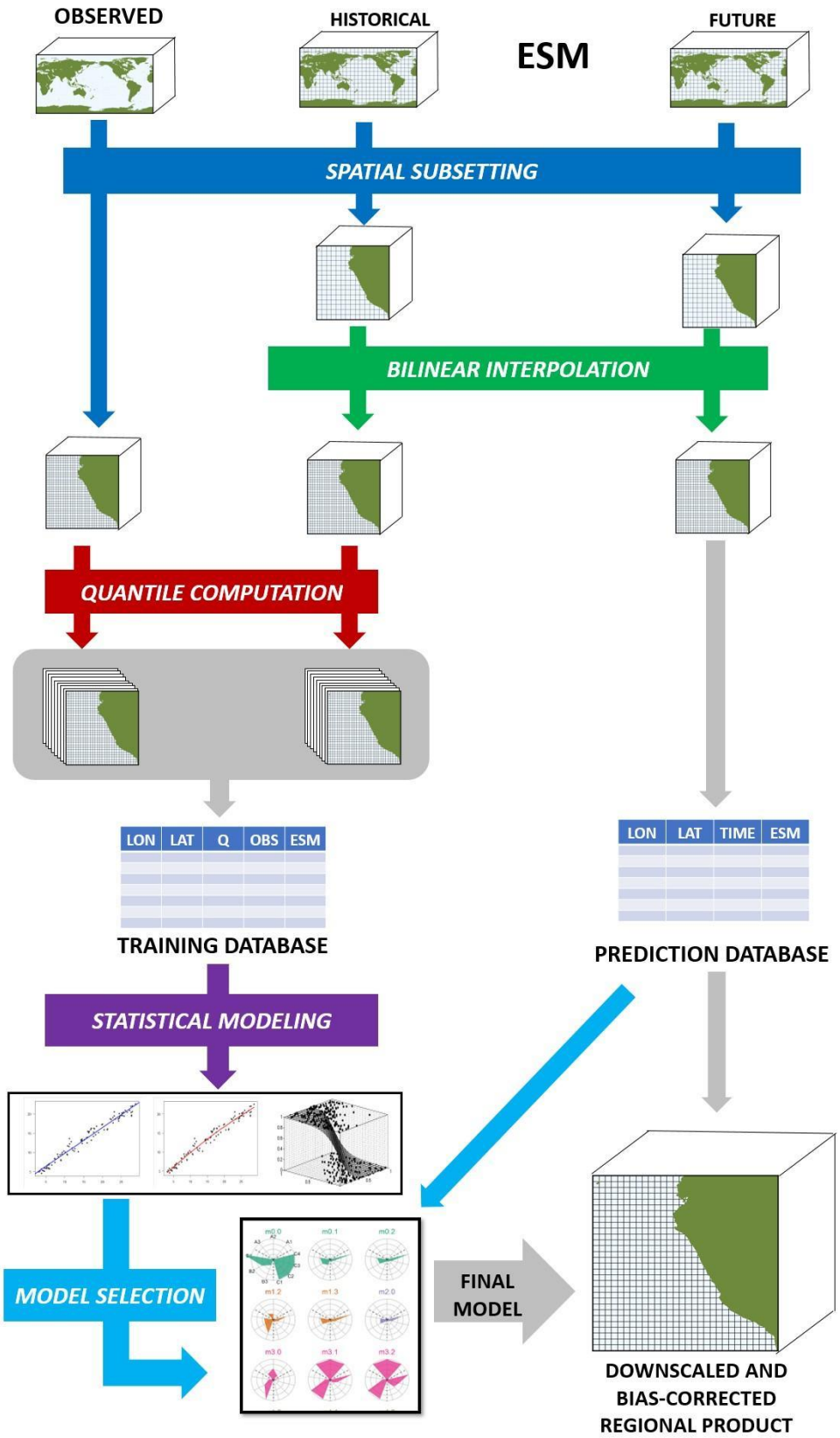

Figure 2. Schematic view of the approach for the statistical downscaling and bias correction protocol. See text for details.

Table 1. Summary of datasets used for the two case studies. n: number of data points. SST: sea surface temperature.

Dataset	n (x10^3)	SST (obs, ºC)		SST (model, ºC)		Distance to coast (km)		Distance to Shelf Break (km)	
		min	max	Min	max	Min	max	min	max
Bay of Biscay and Celtic Sea Ecoregion									
Historical	1014	-0.27	28.35	-1.50	27.72	0	931	-716	987
RCP 2.6	11359			-0.25	30.63	0	931	-716	987
RCP 8.5	11359			-1.37	33.53	0	931	-716	987
RCP 8.5(2090-2100)	100			4.43	31.72	0	931	-716	987
Northern Peru Current Ecosystem									
Historical	950	13.36	30.97	11.66	30.77	1	1866	-1201	1870
RCP 2.6	11359			11.92	31.71	1	1866	-1201	1870
RCP8.5	11359			12.44	34.62	1	1866	-1201	1870
RCP 8.5 (2090-2100)	100			16.47	33.83	1	1866	-1201	1870

2.2 Statistical models

Nineteen nested statistical models (Table 2) describing the relationship between the empirical distributions of historical modeled and observed SST were constructed using Generalized Additive Models (GAM) as implemented in the *mgcv* 1.8-24 R package (Wood 2017) and Shape Constrained Additive models (SCAM, Pya and Wood 2015) as implemented in the scam 1.2-2 R package (Pya 2017), to make use of the monotonicity properties of the relationship between quantiles of ESM and target data, and to avoid overfitting. Some models included spatial covariates (longitude, latitude and distance to the shelf break). The computational complexity of the statistical models selected directly translates into computational costs, but even for the most complex model the fitting time is in the order of magnitude of tens of hours on a multicore computer and minutes for the simplest models.

Models are presented in five groups (Table 2): Group 0 does global bias-correction (i.e. constant throughout the spatial domain) with and without rescaling of SST. Group 1 does also global bias-correction but with additional nonlinear rescaling of SST, allowing for different bias-correction in the distribution tails than in the central range of the temperature. Group 2 models perform spatially explicit bias-correction (i.e. bias-correction varies in space) using linear relationships. Group 3 models are similar to group 2 models but with the difference of more flexible non-linear relationships. Group 4 models present a mix of terms, allowing for linear and non-linear bias corrections.

Table 2. Description of the models tested for bias correcting downscaled predictions. Some models were tested with different smoothing bases for the univariate and the bivariate splines producing different models for the same model equations. Additional covariates (like distance to shelf-break) are included in the "mean" component b(...). The modeled variable (SST here) is represented by x.

Model		Description
0. Global linear		
0.0	$x_{obs} = x + b_0$	Global mean bias correction (NULL model)
0.1	$x_{obs} = x + b(\dots)$	Spatial mean bias correction
0.2	$x_{obs} = a_{11}x + b(\dots)$	Global linear correction
1. Global non-linear		
1.0	$x_{obs} = a_{11}(x) + b(\dots)$	Global non-linear correction
1.1		Global monotonic increasing correction
1.2		Global monotonic increasing and convex correction
1.3		Global monotonic increasing and concave correction
2. Spatially-explicit linear correction		
2.0	$x_{obs} = a_0(lon, lat)x + b(\dots)$	Spatially-varying coefficients
2.1	$x_{obs} = a_{01}(lon)x + a_{02}(lat)x + b(\dots)$	Additive spatially-varying coefficients
2.2	$x_{obs} = (a_{11} + a_{12}lon + a_{13}lat)x + b(\dots)$	Additive linear spatial coefficients
3. Spatially-explicit non-linear correction		
3.0	$x_{obs} = a_{11}(x) + a_{12}(lon, x) + a_{13}(lat, x) + b(\dots)$	Non-linear correction
3.1		Monotonic increasing correction
3.2		Monotonic increasing and convex correction
3.3		Monotonic increasing and concave correction
3.4	$x_{obs} = a_{12}(lon, x) + a_{13}(lat, x) + b(\dots)$	Monotonic increasing correction spatial-only correction
4. Spatially-varying mixed		
4.0	$x_{obs} = a_0(lon, lat)x + a_{11}(x) + a_{12}(lon, x) + a_{13}(lat, x) + b(\dots)$	
4.1	$x_{obs} = a_0(lon, lat)x + a_{12}(lon, x) + a_{13}(lat, x) + b(\dots)$	
4.2	$x_{obs} = a_0(lon, lat)x + a_{11}(x) + b(\dots)$	
4.3	$x_{obs} = a(lon, lat, x) + b(\dots)$	

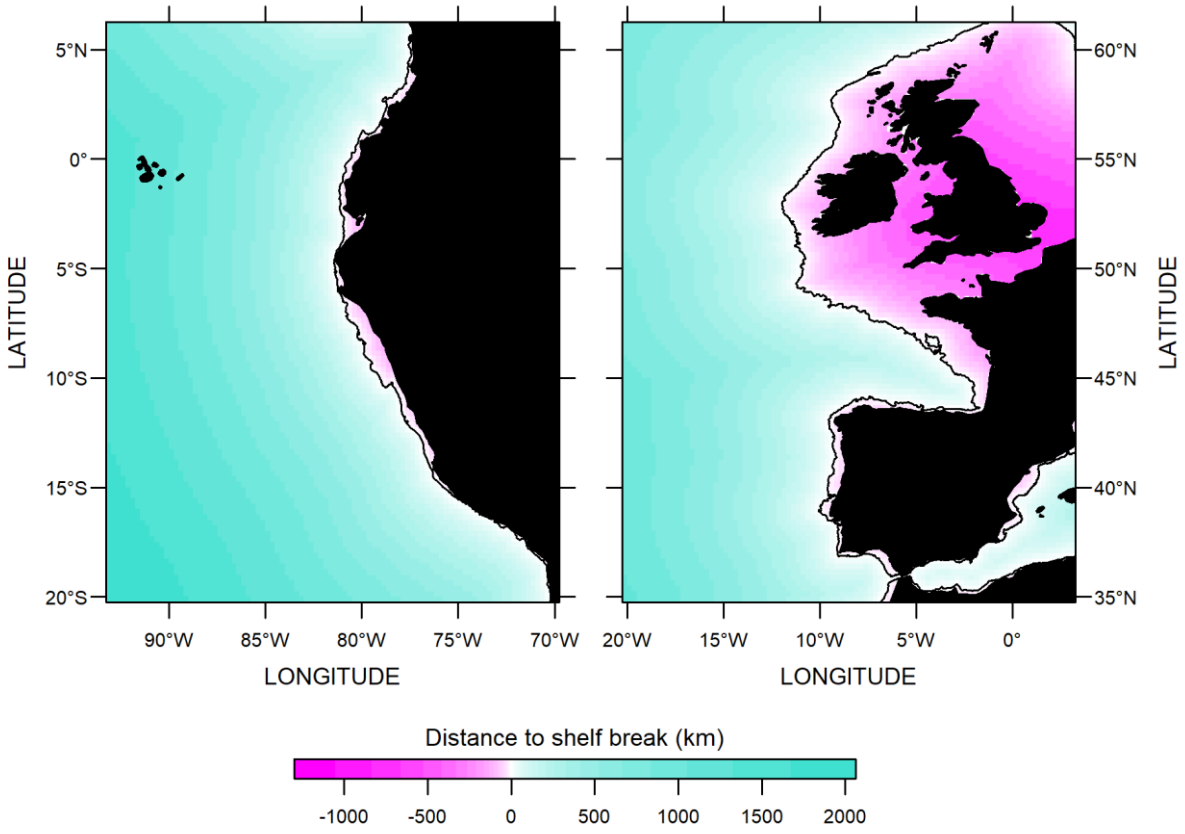

Figure 3. Case study domains showing the distance to the shelf break (purple within the shelf, cyan outside) for the Northern Peru Current Ecosystem (left) and the Ecoregion Bay of Biscay and Celtic Sea (right).

2.3 Model selection

Model selection was based on the comparison of several indicators of predictive performance (Table 3). The performance indicators were grouped into three categories: Future bias indicators (A), residual indicators (B) and deviance indicators (C). The category A indicators measure the relative change in bias between the future and the historical periods, for the minimum, maximum and the whole dataset. The purpose is to identify large deviations in the future predictions, implying a large bias possibly due to overfitting the historical data, which is reported as an issue for bias-correction methods (Cannon et al. 2015). The category B indicators measure the magnitude, range and asymmetry in the residual distribution for the historical data set; they correspond to the more standard test for the performance of regressions. Finally, the category C indicators measure the unexplained deviance of the model for the full dataset and some selected subsets (inside the shelf-break, minimum and maximum temperature) that normally represents a challenge for statistical downscaling methods (Hempel et al. 2013).

The indicators were calculated for each of the 24 models fitted to each data subset, and the 95% percentile was used for a first screening of model performance. After that step, the best models for each case study were fitted to the full dataset, and the indicators were calculated again to select the final model (i.e the downscaling model). The downscaling model was applied to the raw future SST and historical scenarios to get the downscaled and bias-corrected SST.

Table 3. Indicators used for model selection.

	Indicator	Range	Description
A. FUTURE BIAS INDICATORS			
A1	Relative change in bias range future vs. present (minima)	[-1,+Inf)	The range of the future bias is divided by the range of the present minus one, for each indicated subset. For visualization purposes, this indicator is normalized over [0, 1]
A2	Relative change in bias range future vs. present (full)	[-1,+Inf)	
A3	Relative change in bias range future vs. present (maxima)	[0,+Inf)	
B. RESIDUAL INDICATORS			
B1	Average magnitude of residuals	[0,+Inf)	Average of the absolute value of all residuals for each tested model.
B2	Range of the residuals	[0,+Inf)	Difference between the maximum and the minimum residuals.
B3	Asymmetry in residual distribution	[0,+Inf)	Zero is the best possible value, for a symmetric distribution of residuals. This indicator detects extrapolation errors in the minimum and maximum. For visualization purposes, this indicator is normalized over the maximum observed value across models.
C. DEVIANCE INDICATORS			
C1	1 - Explained Deviance, full dataset	[0,1]	Explained deviance proportion was calculated for each subset using the constant bias model (0.0) as null model. One minus the explained deviance was used as an indicator to make zero the best possible value.
C2	1 - Explained Deviance, extrapolation (shelf).	[0,1]	
C4	1 - Explained Deviance, quantile=0% (minima)	[0,1]	
C7	1 - Explained Deviance, quantile=100% (maxima)	[0,1]	

3. Results

The indicators calculated during the cross-validation are shown in Figures 4 and 5 for the Bay of Biscay-Celtic Sea and the northern Peru Current ecosystem, respectively. The group 0 models did not produce extrapolation issues (category A indicators) but performed poorly concerning the distribution of residuals and explained deviance (categories B and C indicators). The group 1 models generally outperformed group 0, but in some cases (Peru) performed poorly for the explained deviance (category C) of the extremes and produced extrapolation problems (category A). The group 2 models performed better than group 1 models, with model 2.0 being the best of the group. Model 2.0 was the closest to apply a regular point-based bias-correction procedure using linear regression but took into account spatial auto-correlation in the slopes of the linear predictors, a feature which is needed when working with gridded data. Models 3.1-3.4 produced extrapolation issues (A indicators), while performing well in explaining the deviance of the extremes in the Bay of Biscay-Celtic Sea case but not in the northern Peru Current case. Model 3.0 performed best within the group 3 models but showed a different behavior for each case study. Group 4 models showed different behaviors for the two case studies, 4.3 showing the worst performance within the group, especially for type A indicators (future projections). Model 4.2 performed the best, especially for category C indicators (spatial extrapolation and extreme values). Based on these results we can report that i) the results of the indicators varied between case studies and ii) that using traditional indicators for statistical model selection only (categories B and C indicators) may select models that increase the bias in future projections (as revealed by category A indicators). The latter point is particularly important as the objective of the statistical model is not to predict the historical period but to produce unbiased downscaled scenarios of the future.

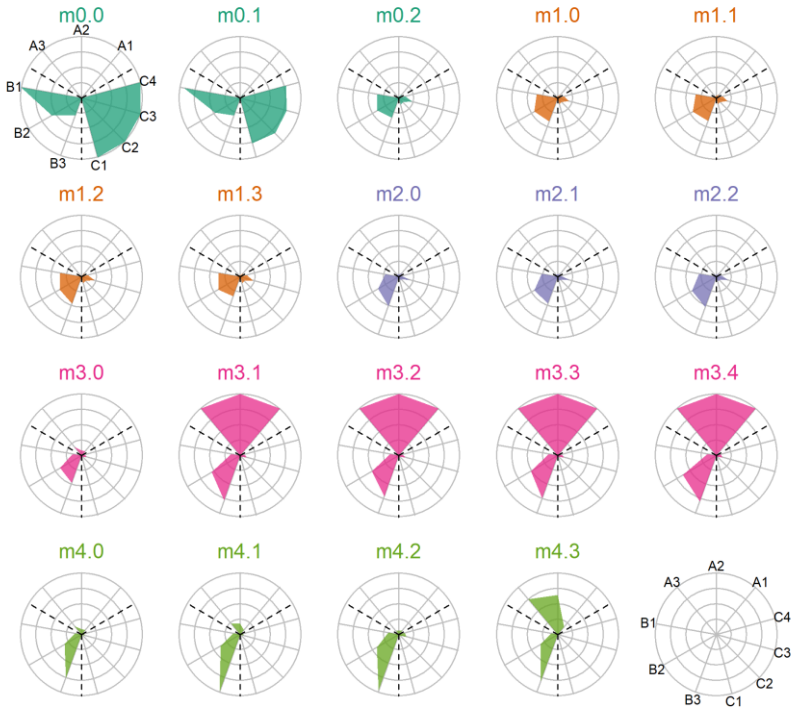

Figure 4. Standardized indicators of model performance for three categories (A, B and C indicators, delimited by dashed lines). Each radar plot represents a statistical downscaling model (m0.0 to m4.3) applied to the Bay of Biscay-Celtic Sea case study. The performance of a model is inversely proportional to the shaded area. See table 2 for model descriptions and table 3 for indicators.

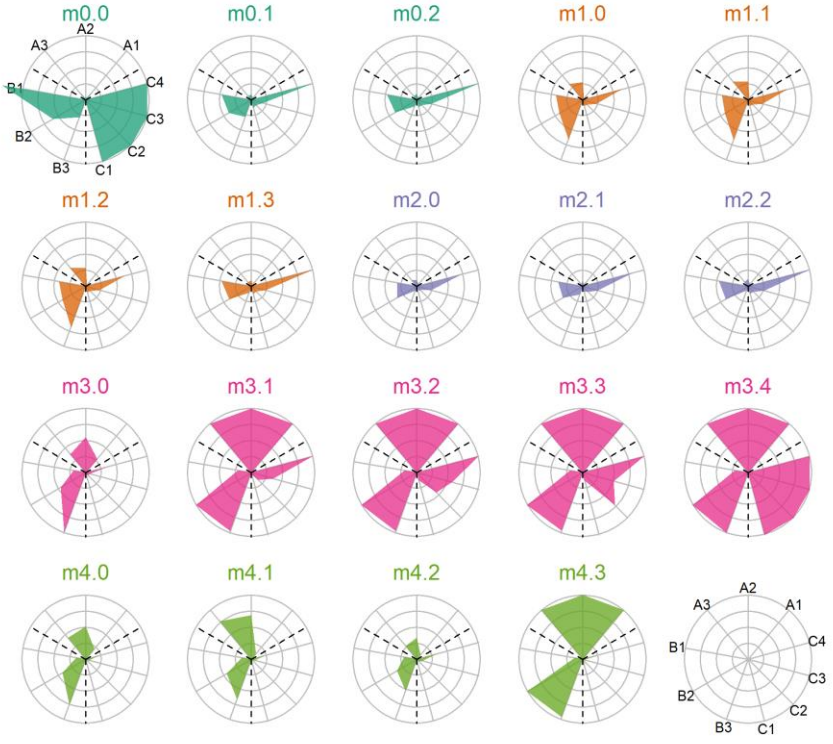

Figure 5. Standardized indicators of model performance for three categories (A, B and C indicators, delimited by dashed lines). Each radar plot represents a statistical downscaling model (m0.0 to m4.3) applied to the northern Peru Current case study. The performance of a model is inversely proportional to the shaded area. See table 2 for model descriptions and table 3 for indicators.

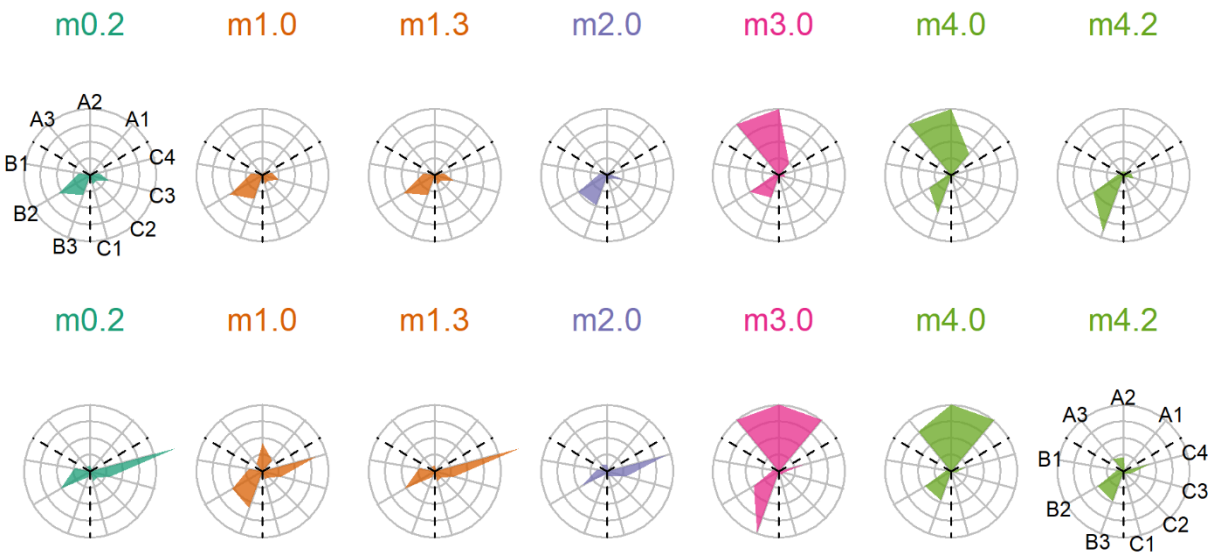

Figure 6. Indicators of performance for the seven models selected for the final screening for the Bay of Biscay-Celtic Sea (top) and the northern Peru Current ecosystem (bottom), using the full dataset. See table 2 for model descriptions and table 3 for indicators.

For the final comparison, models 0.2, 1.0, 1.3, 2.0, 3.0, 4.0 and 4.2 were used (Figure 6), corresponding to the best models of each group for the two case studies. In this final assessment, the best two models according to our indicators were models 2.0 and 4.2, for both case studies. For the northern Peru Current case study, the results were less clear for the distinction between models 2.0 and 4.2, as model 2.0 performed better for category B indicators but worse for category C indicators.

When predicting models 2.0 and 4.2 for different quantiles (minimum, 5%, 95% and maximum) and the mean of the historical period (Figure 7) we observed that model 4.2 performed better within the 5-95% range but the direction of the bias changed for the extremes (maximum and minimum), especially for the northern Peru Current system, suggesting an overfitting of that model for this case study.

In Figure 8, the logarithm of the ratio of the absolute value of the residuals after downscaling and bias correction between models 4.2 and 2.0 is depicted, showing spatial differences in the prediction skills for the extreme values of the SST distribution. In addition, the spatial patterns predicted by these two models were different for the minima and the maxima of SST. For example, for the maximum temperature in the Peru case study, model 4.2 tended to perform better, especially in the coastal and northern areas. However, model 4.2 showed a positive bias for the maximum temperature (Figure 7) that may artificially enhance the rise of temperature as shown in Figure 9. When aggregating the results over the whole case study domains, no differences were observed between model 2.0 and 4.2 for the Bay of Biscay-Celtic Sea case. In contrast, for the northern Peru Current case the results showed that model 4.2 produced slightly warmer temperatures for the RCP 2.6 scenario but much higher temperatures for the RCP 8.5 scenario, surpassing even the original ESM predictions (Figure 9). However, both statistical downscaling models were able to bias-correct the original ESMs outputs as the predictions were now inside the original range of SST variability (orange rectangles in Figure 9). These results highlight the importance of including the category A indicators for model selection, as they help detect this type of issue that compromise the capability of the statistical downscaling to produce plausible future scenarios results.

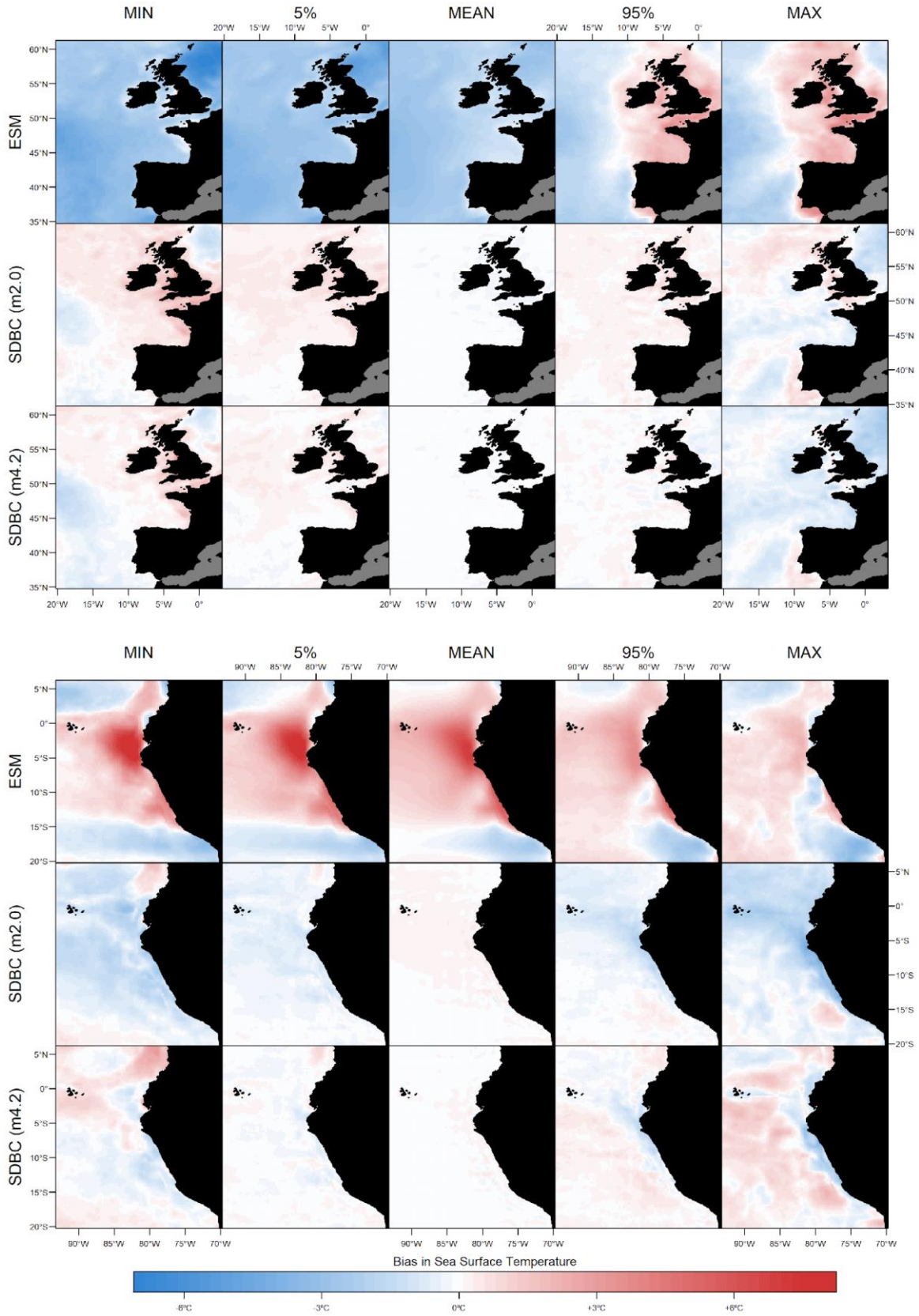

Figure 7. Comparison of absolute bias in the minimum, 5% quantile, mean, 95% quantile and maximum sea surface temperature. Panel A (top) shows the results for the Bay of Biscay-Celtic Sea and panel B (bottom) for the northern Peru Current system. In each panel, the top row shows the bias of the IPSL-CM5A-LR after a bilinear interpolation and the intermediate and bottom rows the bias after downscaling and bias correction using model m2.0 and m4.2, respectively. The columns present the minimum, 5% quantile, mean, 95% quantile and maximum from left to right.

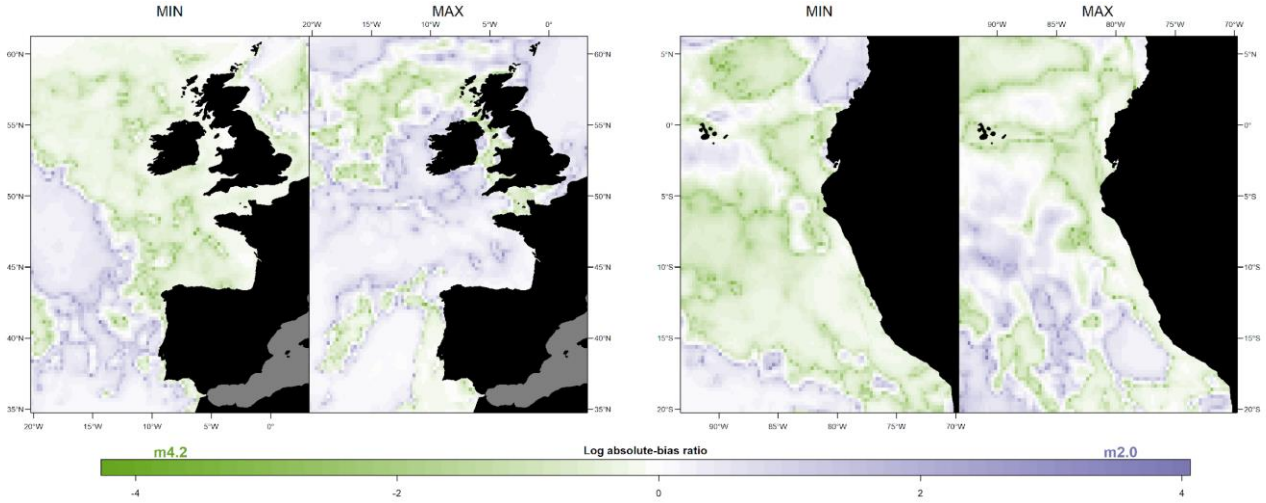

Figure 8. Log absolute-bias ratio between models 4.2 (green) and 2.0 (purple) for the Bay of Biscay-Celtic Sea (left) and the northern Peru Current system (right). The intensity of the color represents how much better each model performed in that particular region in terms of reducing the bias between the downscaled and bias-corrected predictions and the target data.

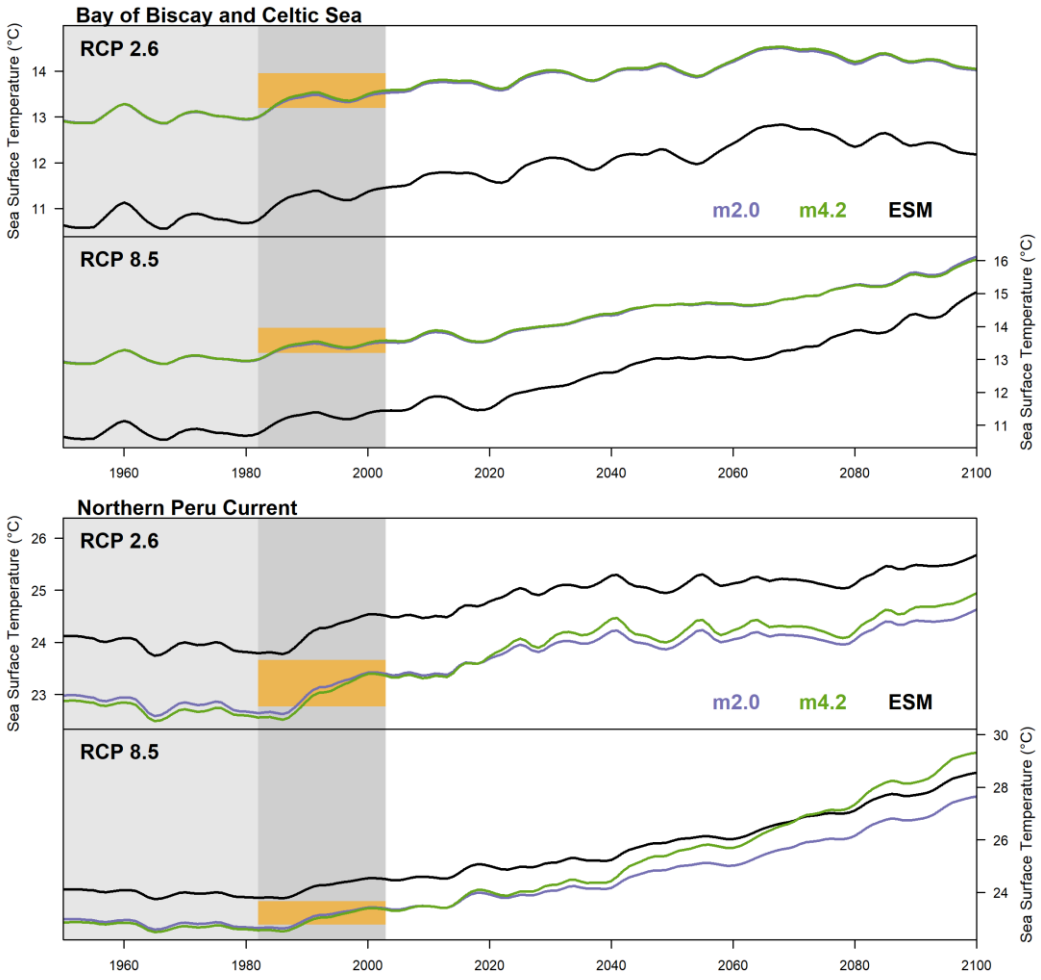

Figure 9. Projected average sea surface temperature under RCP 2.6 and RCP 8.5 scenarios for the two case studies. The average sea surface temperature after downscaling and bias correction (color lines) is compared to the original IPSL-CM5A-LR ESM outputs (black line). The range of observed variability is shown by the orange rectangle. In the Bay of Biscay and Celtic Sea model m2.0 and m4.2 results overlap.

4. Conclusions

The application of our approach to two different case studies showed that the performance of statistical downscaling models is difficult to generalize across regions and it should therefore be evaluated for each case. The multi-model comparison is a strength of our approach and additional models could be included in the original ensemble of models (e.g., including different spatial covariates). A formal statistical procedure including validation and model selection is encouraged to produce outputs downscaling that are reliable for regional applications. Another important feature of our approach is the evaluation of not only the capacity of the models to preserve temporal patterns (e.g., temporal trends) but also spatial patterns. The latter aspect is particularly important when extrapolation to coastal regions that are not covered by the ESMs is needed.

Acknowledgements

YJS and ROR acknowledge funding support from the Biodiversa and Belmont Forum project SOMBEE (BiodivScen ERA-Net COFUND programme, ANR contract n°ANR-18-EBI4-0003-01), the European Union's Horizon 2020 research and innovation programme under grant agreement No 817578 (TRIATLAS). ROR was also funded by the IMARPE-PRODUCE-IADB Project "Adaptation to climate change of the fishery sector and marine-coastal ecosystem of Perú" (PE-G1001/PE-T1297) and the PrimeTradeOffs project (ERA-NET COFASP programme, ANR-15-COFA-0004-01). YJS was also funded through the European Union's Horizon 2020 research and innovation programme under grant agreement No 869300 (FutureMARES) and the Pew marine fellows programme. VT was funded by the European Union under the Horizon Europe RIA program (NECCTON, grant agreement 101081273). The authors would like to thank the Pôle de Calcul et de Données Marines (PCDM) for providing access to their DATARMOR computing resources (https://wwz.ifremer.fr/pcdm/Equipement).

Open Research

The R scripts used to execute the analyses in the paper can be found at https://github.com/roliveros-ramos/sdbc/tree/paper, and are preserved at DOI:10.5281/zenodo.7694472. The climate change simulations used for the study are available at https://data.isimip.org/.

References

Araya-Osses, D., Casanueva, A., Román-Figueroa, C., Uribe, J. M., & Paneque, M. (2020). Climate change projections of temperature and precipitation in Chile based on statistical downscaling. Climate Dynamics, 54(9–10), 4309–4330. https://doi.org/10.1007/s00382-020-05231-4

Asong, Z. E., Khaliq, M. N., & Wheater, H. S. (2016). Projected changes in precipitation and temperature over the Canadian Prairie Provinces using the Generalized Linear Model statistical downscaling approach. Journal of Hydrology, 539, 429–446. https://doi.org/10.1016/j.jhydrol.2016.05.044

Baño-Medina, J., Manzanas, R., & Gutiérrez, J. M. (2020). Configuration and intercomparison of deep learning neural models for statistical downscaling. Geoscientific Model Development, 13(4), 2109–2124. https://doi.org/10.5194/gmd-13-2109-2020

Bonafoni, S., Anniballe, R., Gioli, B., & Toscano, P. (2016). Downscaling Landsat Land Surface Temperature over the urban area of Florence. European Journal of Remote Sensing, 49(1), 553–569. https://doi.org/10.5721/EuJRS20164929

Cannon, A. J., Sobie, S. R., & Murdock, T. Q. (2015). Bias Correction of GCM Precipitation by Quantile Mapping: How Well Do Methods Preserve Changes in Quantiles and Extremes? Journal of Climate, 28(17), 6938–6959. https://doi.org/10.1175/JCLI-D-14-00754.1

Fowler, H. J., Blenkinsop, S., & Tebaldi, C. (2007). Linking climate change modelling to impacts studies: Recent advances in downscaling techniques for hydrological modelling: ADVANCES IN DOWNSCALING TECHNIQUES FOR HYDROLOGICAL MODELLING. International Journal of Climatology, 27(12), 1547–1578. https://doi.org/10.1002/joc.1556

González-Aparicio, I., Monforti, F., Volker, P., Zucker, A., Careri, F., Huld, T., & Badger, J. (2017). Simulating European wind power generation applying statistical downscaling to reanalysis data. Applied Energy, 199, 155–168. https://doi.org/10.1016/j.apenergy.2017.04.066

Han, Z., Shi, Y., Wu, J., Xu, Y., & Zhou, B. (2019). Combined Dynamical and Statistical Downscaling for High-Resolution Projections of Multiple Climate Variables in the Beijing–Tianjin–Hebei Region of China. Journal of Applied Meteorology and Climatology, 58(11), 2387–2403. https://doi.org/10.1175/JAMC-D-19-0050.1

He, X., Chaney, N. W., Schleiss, M., & Sheffield, J. (2016). Spatial downscaling of precipitation using adaptable random forests. Water Resources Research, 52(10), 8217–8237. https://doi.org/10.1002/2016WR019034

Hempel, S., Frieler, K., Warszawski, L., Schewe, J., & Piontek, F. (2013). A trend-preserving bias correction – the ISI-MIP approach. Earth System Dynamics, 4(2), 219–236. https://doi.org/10.5194/esd-4-219-2013

Hertig, E., & Tramblay, Y. (2017). Regional downscaling of Mediterranean droughts under past and future climatic conditions. Global and Planetary Change, 151, 36–48. https://doi.org/10.1016/j.gloplacha.2016.10.015

Hoomehr, S., Schwartz, J. S., & Yoder, D. C. (2016). Potential changes in rainfall erosivity under GCM climate change scenarios for the southern Appalachian region, USA. CATENA, 136, 141–151. https://doi.org/10.1016/j.catena.2015.01.012

Hoskins, A. J., Bush, A., Gilmore, J., Harwood, T., Hudson, L. N., Ware, C., Williams, K. J., & Ferrier, S. (2016). Downscaling land-use data to provide global 30″ estimates of five land-use classes. Ecology and Evolution, 6(9), 3040–3055. https://doi.org/10.1002/ece3.2104

Huang, Y. F., Ang, J. T., Tiong, Y. J., Mirzaei, M., & Amin, M. Z. M. (2016). Drought Forecasting Using SPI and EDI under RCP-8.5 Climate Change Scenarios for Langat River Basin, Malaysia. Procedia Engineering, 154, 710–717. https://doi.org/10.1016/j.proeng.2016.07.573

Keller, J. D., Delle Monache, L., & Alessandrini, S. (2017). Statistical Downscaling of a High-Resolution Precipitation Reanalysis Using the Analog Ensemble Method. Journal of Applied Meteorology and Climatology, 56(7), 2081–2095. https://doi.org/10.1175/JAMC-D-16-0380.1

Lange, S. (2019). Trend-preserving bias adjustment and statistical downscaling with ISIMIP3BASD (v1.0). Geoscientific Model Development, 12(7), 3055–3070. https://doi.org/10.5194/gmd-12-3055-2019

Lanzante, J. R., Dixon, K. W., Nath, M. J., Whitlock, C. E., & Adams-Smith, D. (2018). Some Pitfalls in Statistical Downscaling of Future Climate. Bulletin of the American Meteorological Society, 99(4), 791–803. https://doi.org/10.1175/BAMS-D-17-0046.1

Latombe, G., Burke, A., Vrac, M., Levavasseur, G., Dumas, C., Kageyama, M., & Ramstein, G. (2018). Comparison of spatial downscaling methods of general circulation model results to study climate variability during the Last Glacial Maximum. Geoscientific Model Development, 11(7), 2563–2579. https://doi.org/10.5194/gmd-11-2563-2018

Morales-Barbero, J., & Vega-Álvarez, J. (2019). Input matters matter: Bioclimatic consistency to map more reliable species distribution models. Methods in Ecology and Evolution, 10(2), 212–224. https://doi.org/10.1111/2041-210X.13124

Oh, M., Lee, J., Kim, J., & Kim, H. (2022). Machine learning-based statistical downscaling of wind resource maps using multi-resolution topographical data. Wind Energy, 25(6), 1121–1141. https://doi.org/10.1002/we.2718

Poggio, L., Simonetti, E., & Gimona, A. (2018) Enhancing the WorldClim data set for national and regional applications. Science of the Total Environment, 625: 1628-1643.

Pourmokhtarian, A., Driscoll, C. T., Campbell, J. L., Hayhoe, K., & Stoner, A. M. K. (2016). The effects of climate downscaling technique and observational data set on modeled ecological responses. Ecological Applications, 26(5), 1321–1337. https://doi.org/10.1890/15-0745

Rheuban, J. E., Kavanaugh, M. T., & Doney, S. C. (2017) Implications of Future Northwest Atlantic Bottom Temperatures on the American Lobster (Homarus americanus) Fishery. Journal of Geophysical Research-Oceans, 122: 9387-9398.

Sa'adi, Z., Shahid, S., Chung, E.-S., & Ismail, T. bin. (2017). Projection of spatial and temporal changes of rainfall in Sarawak of Borneo Island using statistical downscaling of CMIP5 models. Atmospheric Research, 197, 446–460. https://doi.org/10.1016/j.atmosres.2017.08.002

Skogen, M. D., Hjollo, S. S., Sando, A. B., & Tjiputra, J. (2018) Future ecosystem changes in the Northeast Atlantic: a comparison between a global and a regional model system. ICES Journal of Marine Science, 75: 2355-2369.

Stoklosa, J., Daly, C., Foster, S. D., Ashcroft, M. B., & Warton, D. I. (2015). A climate of uncertainty: Accounting for error in climate variables for species distribution models. Methods in Ecology and Evolution, 6(4), 412–423. https://doi.org/10.1111/2041-210X.12217

Su, B., Huang, J., Gemmer, M., Jian, D., Tao, H., Jiang, T., & Zhao, C. (2016). Statistical downscaling of CMIP5 multi-model ensemble for projected changes of climate in the Indus River Basin. Atmospheric Research, 178–179, 138–149. https://doi.org/10.1016/j.atmosres.2016.03.023

Tabor, K., & Williams, J. W. (2010). Globally downscaled climate projections for assessing the conservation impacts of climate change. Ecological Applications, 20(2), 554–565. https://doi.org/10.1890/09-0173.1

Teutschbein, C., & Seibert, J. (2012). Bias correction of regional climate model simulations for hydrological climate-change impact studies: Review and evaluation of different methods. Journal of Hydrology, 456–457, 12–29. https://doi.org/10.1016/j.jhydrol.2012.05.052

Townhill, B., Pinnegar, J., Tinker, J., Jones, M., Simpson, S., Stebbing, P., & Dye, S. (2017) Non-native marine species in north-west Europe: Developing an approach to assess future spread using regional downscaled climate projections. Aquatic Conservation-Marine and Freshwater Ecosystems, 27: 1035-1050.

Volosciuk, C., Maraun, D., Vrac, M., & Widmann, M. (2017). A combined statistical bias correction and stochastic downscaling method for precipitation. Hydrology and Earth System Sciences, 21(3), 1693–1719. https://doi.org/10.5194/hess-21-1693-2017

Wang, C., Zhang, L., Lee, S.-K., Wu, L., & Mechoso, C. R. (2014). A global perspective on CMIP5 climate model biases. Nature Climate Change, 4(3), 201–205. https://doi.org/10.1038/nclimate2118

Wang, T., Hamann, A., Spittlehouse, D., & Carroll, C. (2016). Locally Downscaled and Spatially Customizable Climate Data for Historical and Future Periods for North America. PLOS ONE, 11(6), e0156720. https://doi.org/10.1371/journal.pone.0156720

Werner, A. T., & Cannon, A. J. (2016). Hydrologic extremes – an intercomparison of multiple gridded statistical downscaling methods. Hydrology and Earth System Sciences, 20(4), 1483–1508. https://doi.org/10.5194/hess-20-1483-2016

Wood, S.N. (2017) Generalized Additive Models: An Introduction with R (2nd edition). Chapman and Hall/CRC.

Wong, G., Maraun, D., Vrac, M., Widmann, M., Eden, J. M., & Kent, T. (2014). Stochastic Model Output Statistics for Bias Correcting and Downscaling Precipitation Including Extremes. Journal of Climate, 27(18), 6940–6959. https://doi.org/10.1175/JCLI-D-13-00604.1

Xu, C. (n.d.). From GCMs to river flow: A review of downscaling methods and hydrologic modelling approaches.

Yue, T., Zhao, N., Fan, Z., Li, J., Chen, C., Lu, Y., Wang, C., Xu, B., & Wilson, J. (2016). CMIP5 downscaling and its uncertainty in China. Global and Planetary Change, 146, 30–37. https://doi.org/10.1016/j.gloplacha.2016.09.003

Zhang, L., Xu, Y., Meng, C., Li, X., Liu, H., & Wang, C. (2020). Comparison of Statistical and Dynamic Downscaling Techniques in Generating High-Resolution Temperatures in China from CMIP5 GCMs. Journal of Applied Meteorology and Climatology, 59(2), 207–235. https://doi.org/10.1175/JAMC-D-19-0048.1